Utilizing Photoionization Efficiency Spectroscopy and Density Functional Theory to Investigate Charge Transfer Interactions in $AuCe_3O_n$ Clusters

Robert A. Hardy, Aidan M. Karayilan and Gregory F. Metha*

Department of Chemistry, The University of Adelaide, South Australia 5005, Australia

Supporting Information

This document contains the following supporting information figures:

Figure S1 and S2: Photoionization mass spectra for $AuCe_mO_n$ and Ce_mO_n clusters, respectively.

Figures S3-S14: PIE spectra and DFT-calculated structures for Ce_3O_n and $AuCe_3O_n$ clusters.

Figure S15: Calculated Au, O and CeO_2 bonding energies for Ce_3O_n and $AuCe_3O_n$ clusters.

Figures S16-S29: Calculated neutral and cationic Ce_3O_n and $AuCe_3O_n$ geometries showing bond lengths and structure point groups.

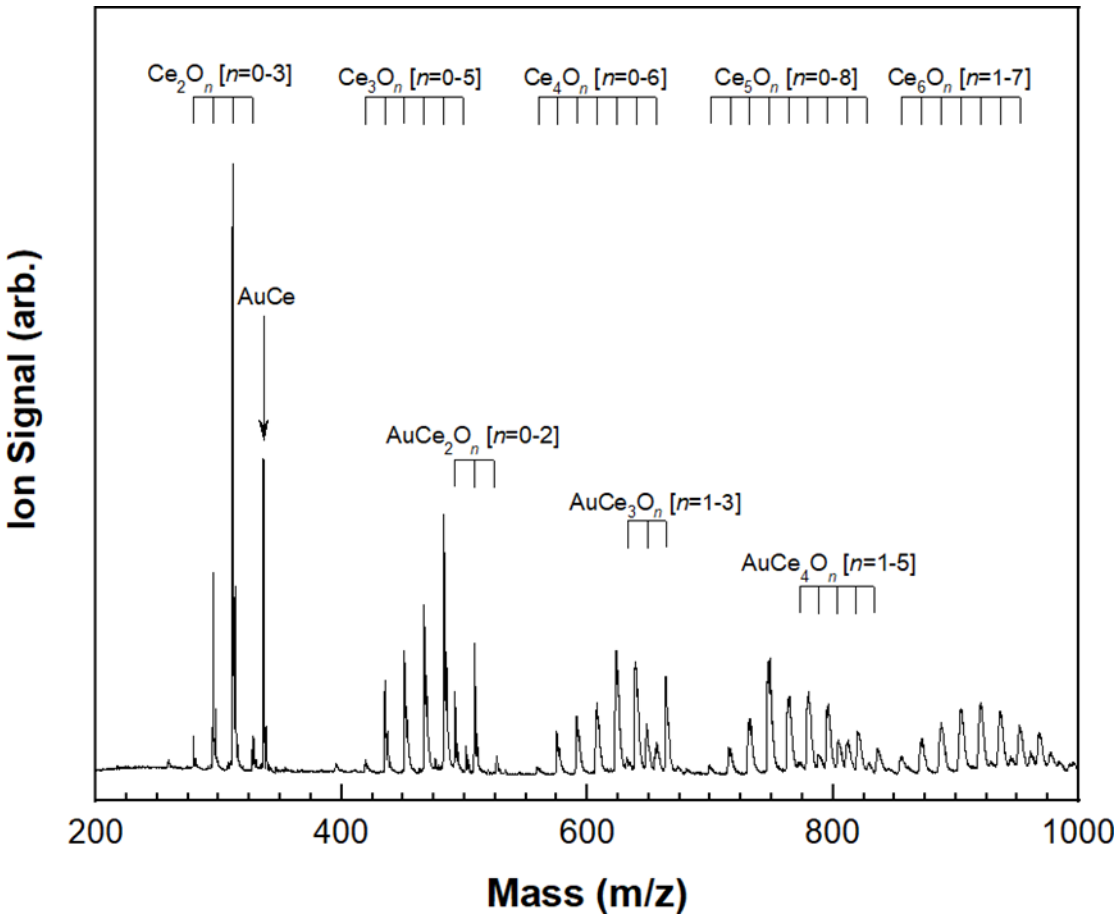

Figure S1: Typical mass spectrum of $AuCe_mO_n^+$ clusters recorded following photoionization at 213 nm (5.82 eV). The $AuCe_mO_n$ and Ce_mO_n ion peaks are labelled with ladders.

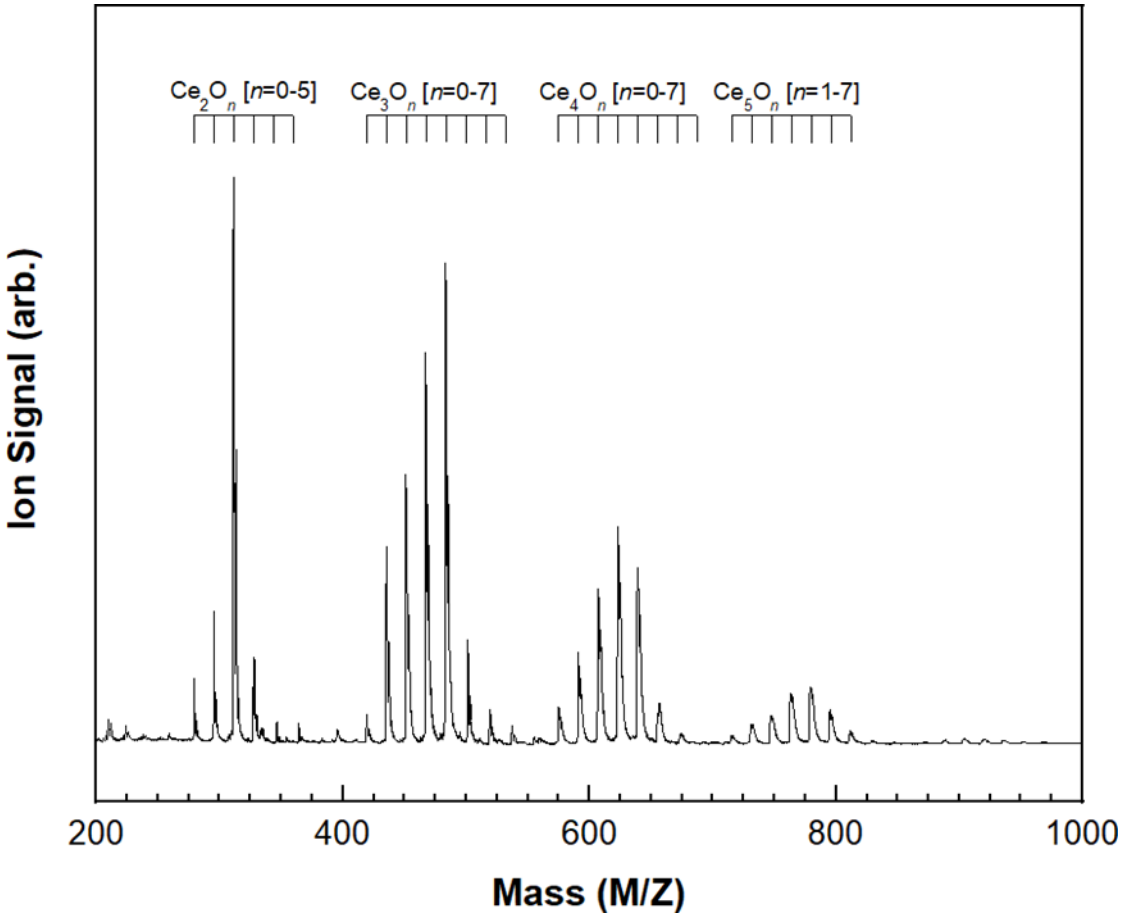

Figure S2: Mass spectrum of $Ce_mO_n^+$ clusters recorded following photoionization at 213 nm (5.82 eV). The Ce_mO_n ion peaks are labelled with ladders.

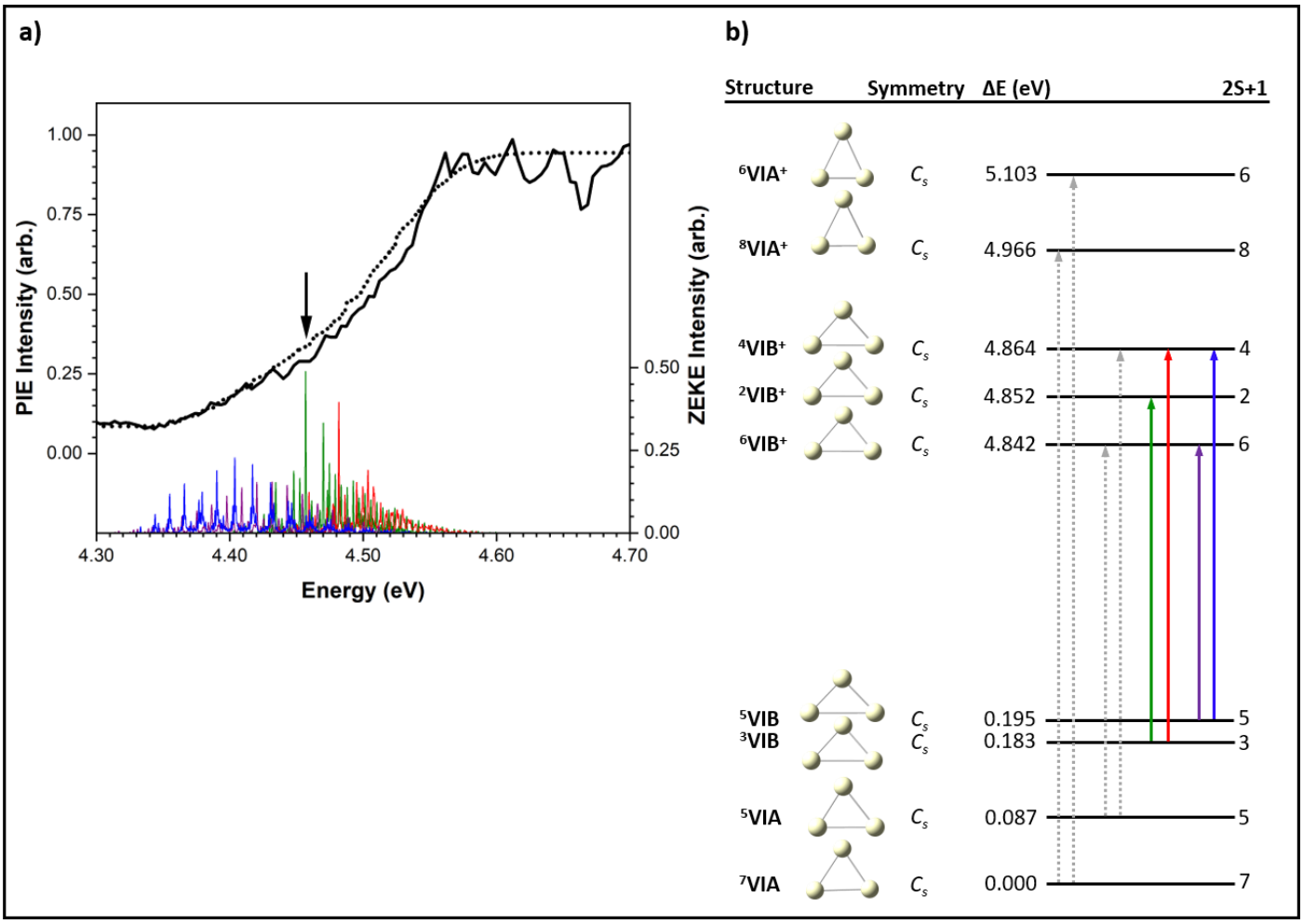

Figure S3: a). PIE spectrum for the Ce_3 cluster. Experimentally recorded and calculated PIE spectra are shown as solid and dotted black lines, respectively. Calculated ZEKE spectra for underlying ionization transitions are shown below the PIE spectra in green, red purple and blue. The downward arrow indicates the adiabatic IE, the lowest energy origin transition. **b).** Calculated Ce_3 structures and ionization processes. Ionization transitions are shown as coloured arrows which correspond to their respective ZEKE spectra. Ionization processes not considered to contribute to the PIE spectrum – due to weak FC overlap - are shown as dotted grey arrows.

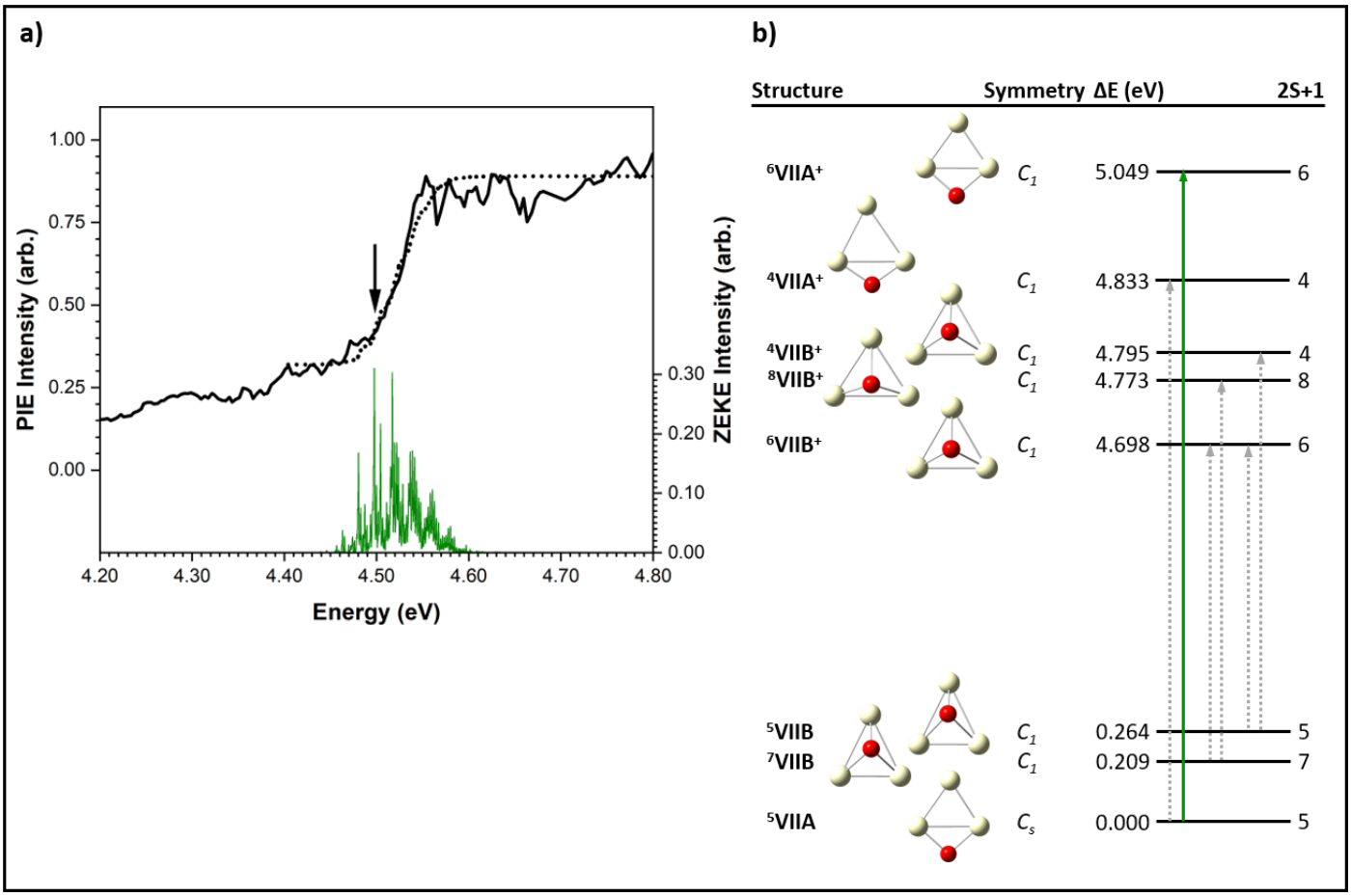

Figure S4: a). PIE spectrum for the Ce_3O cluster. Experimentally recorded and calculated PIE spectra are shown as solid and dotted black lines, respectively. The calculated ZEKE spectrum for the underlying ionization transitions is shown below the PIE spectrum in green. The downward arrow indicates the adiabatic IE, the lowest energy origin transition. **b).** Calculated Ce_3O structures (Ce is white and O is red) and ionization processes. Ionization transitions are shown as coloured arrows which correspond to their respective ZEKE spectra. Ionization processes not considered to contribute to the PIE spectrum – due to weak FC overlap - are shown as dotted grey arrows.

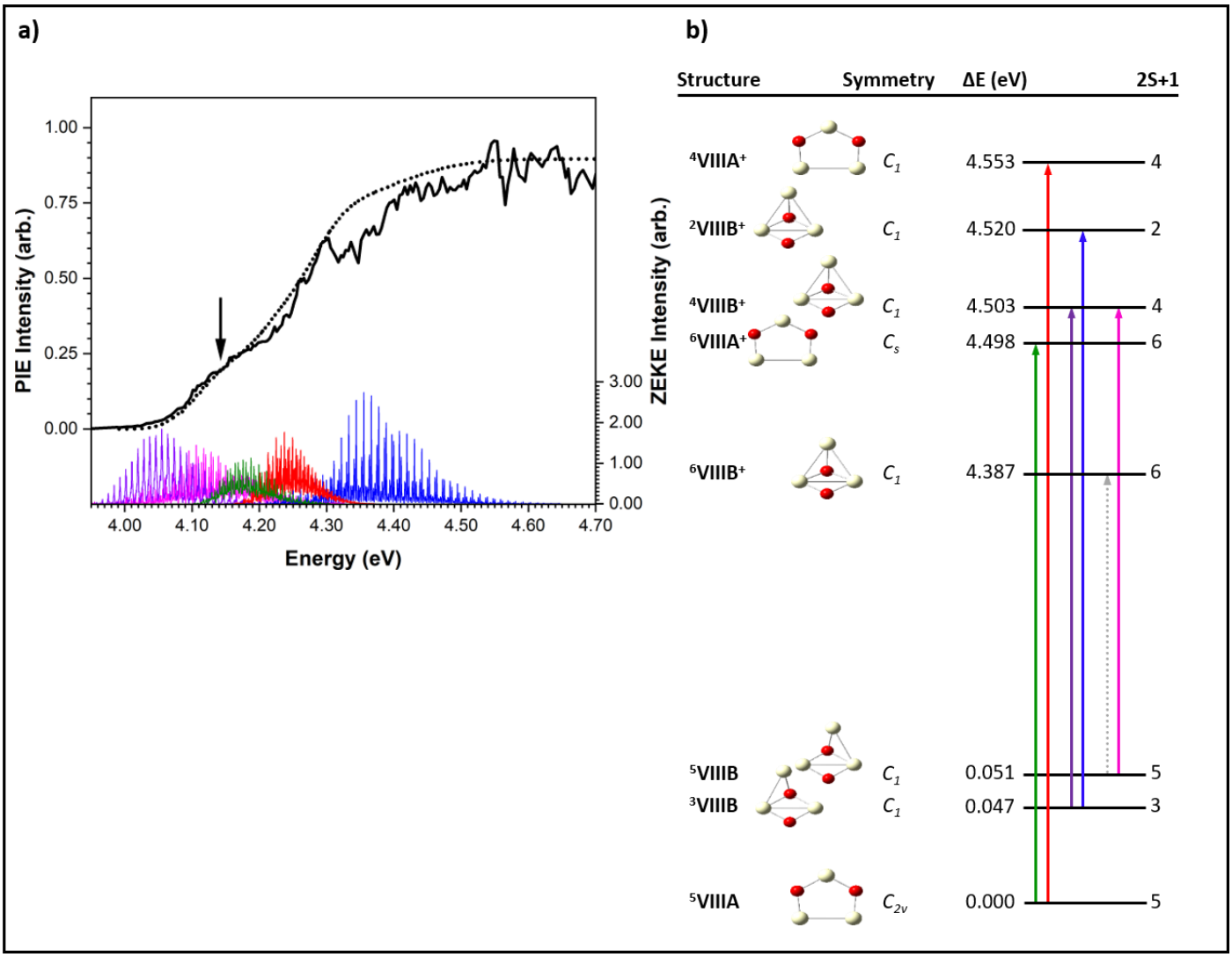

Figure S5: a). PIE spectrum for the Ce_3O_2 cluster. Experimentally recorded and calculated PIE spectra are shown as solid and dotted black lines, respectively. Calculated ZEKE spectra for underlying ionization transitions are shown below the PIE spectrum in green, red, violet, blue and magenta. The downward arrow indicates the adiabatic IE, the lowest energy origin transition. **b).** Calculated Ce_3O_3 structures (Ce is white and O is red) and ionization processes. Ionization transitions are shown as coloured arrows which correspond to their respective ZEKE spectra. Ionization processes not considered to contribute to the PIE spectrum – due to weak FC overlap - are shown as dotted grey arrows.

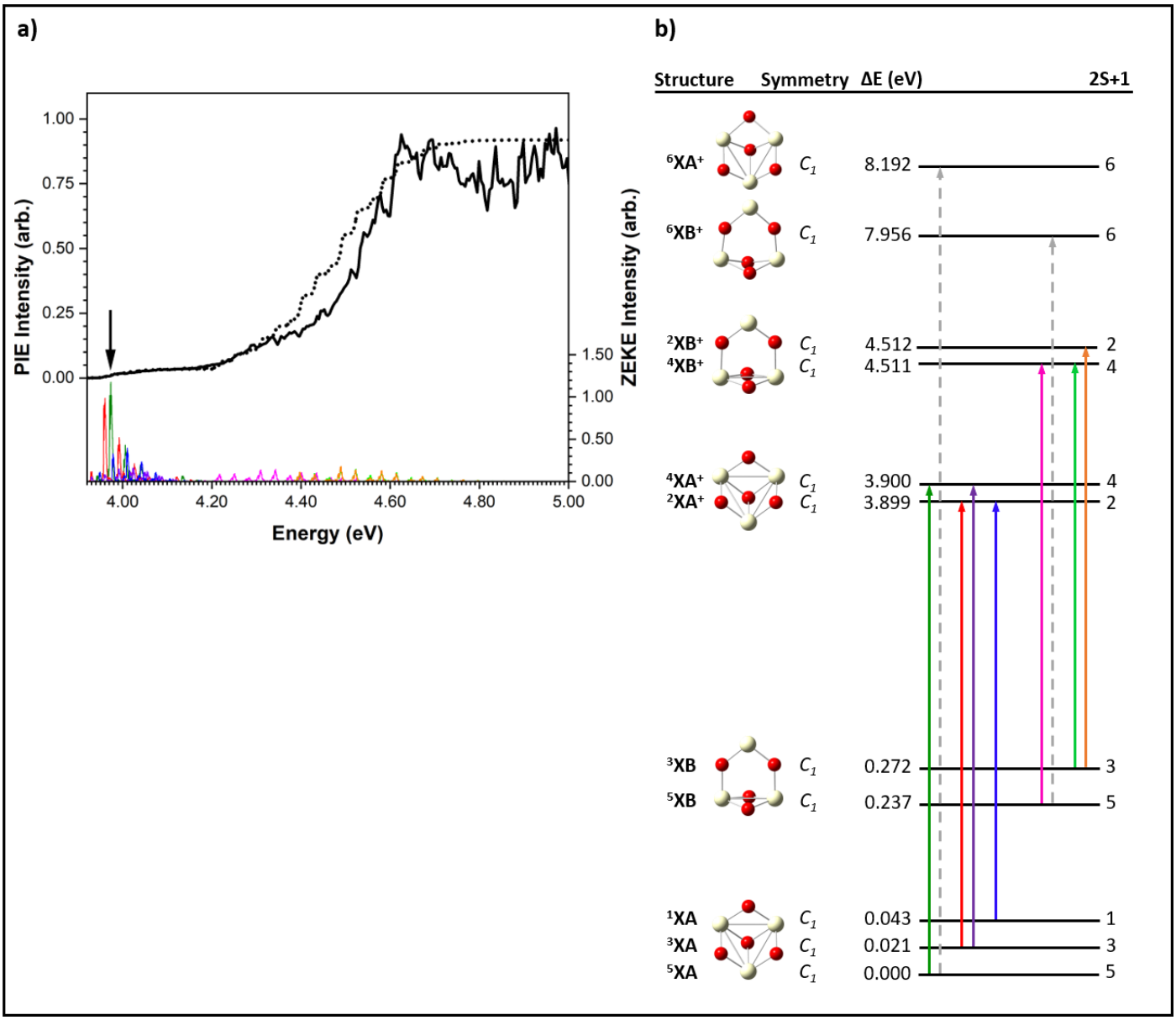

Figure S6: a). PIE spectrum for the Ce_3O_4 cluster. Experimentally recorded and calculated PIE spectra are shown as solid and dotted black lines, respectively. Calculated ZEKE spectra for the underlying ionization transitions are shown below the PIE spectrum in green, red, violet, blue, magenta, lime and orange. The downward arrow indicates the adiabatic IE, the lowest energy origin transition. **b).** Calculated Ce_3O_4 structures (Ce is white and O is red) and ionization processes. Ionization transitions are shown as coloured arrows which correspond to their respective ZEKE spectra. Ionization processes not considered to contribute to the PIE spectrum – due to high ionization energies - are shown as dashed grey arrows.

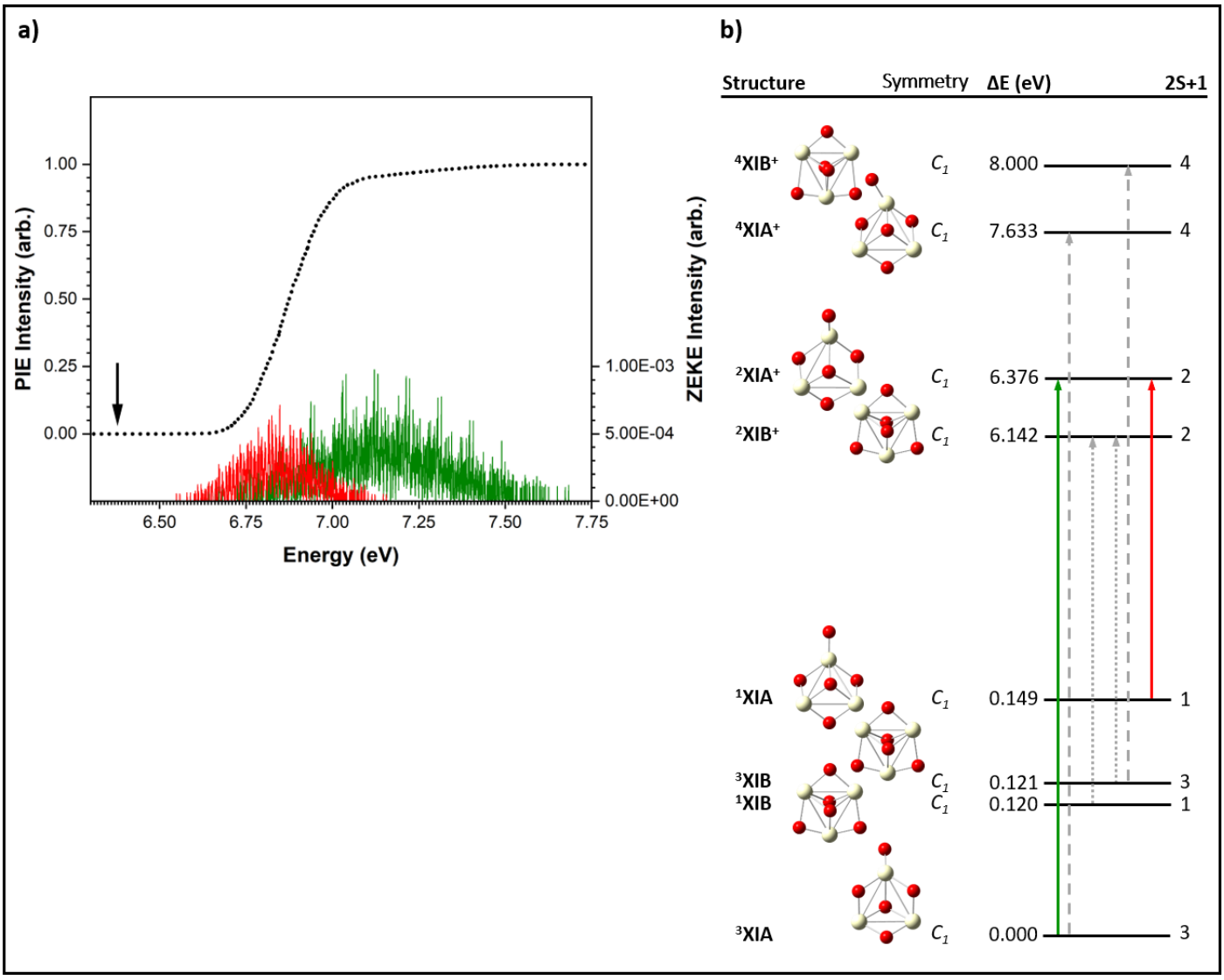

Figure S7: a). PIE spectrum for the Ce_3O_5 cluster. The calculated PIE spectrum is shown as a dotted black line. Calculated ZEKE spectra for the underlying ionization transitions are shown below the PIE spectrum in green and red. The downward arrow indicates the calculated adiabatic IE, the lowest energy origin transition. **b).** Calculated Ce_3O_5 structures (Ce is white and O is red) and ionization processes. Ionization transitions are shown as coloured arrows which correspond to their respective ZEKE spectra. Ionization processes not considered to contribute to the PIE spectrum – due to high ionization energies and weak FC overlap - are shown as dashed grey arrows and dotted grey arrows, respectively.

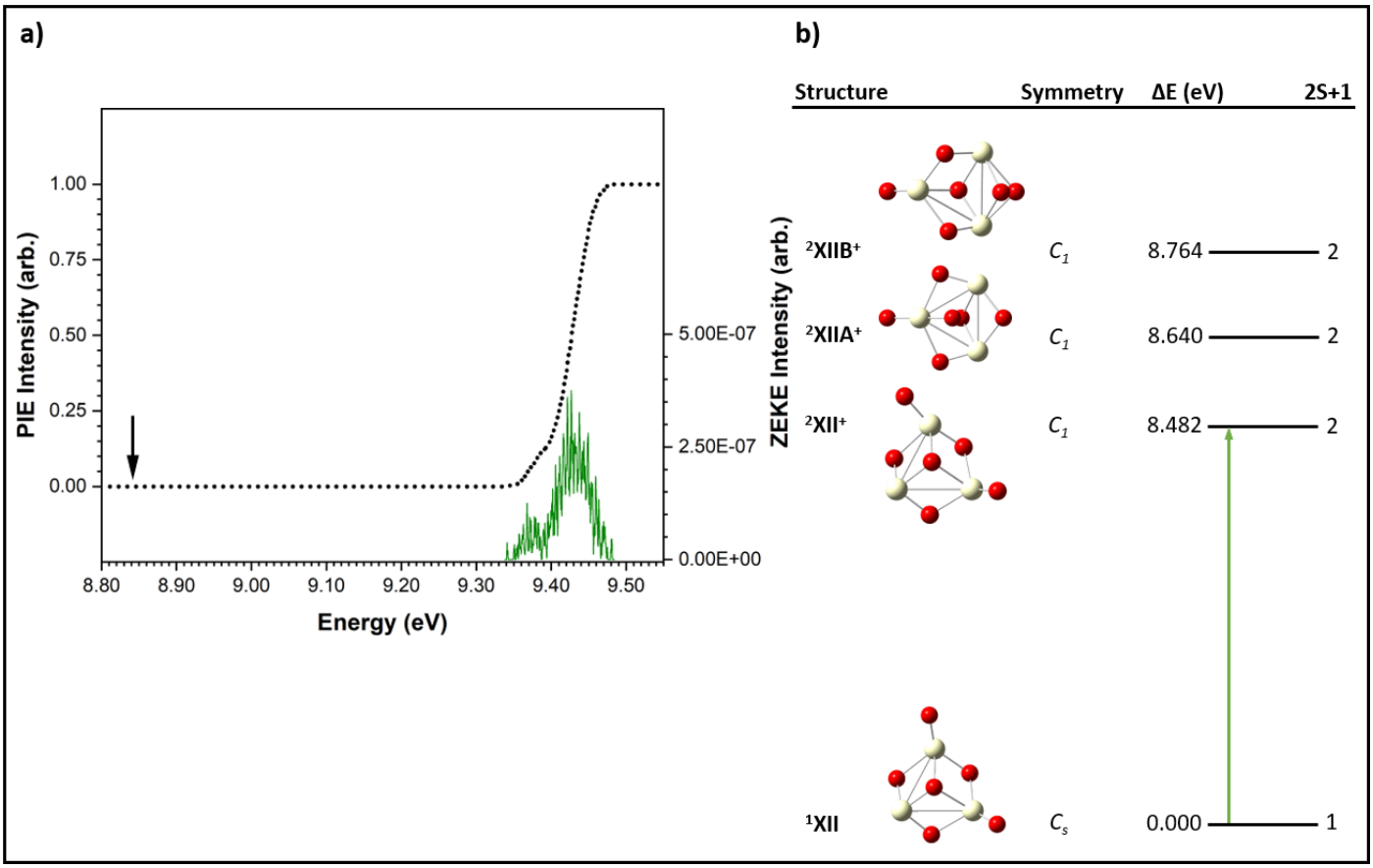

Figure S8: a). PIE spectrum for the Ce_3O_6 cluster. The calculated PIE spectrum is shown as a dotted black line. The calculated ZEKE spectrum for the underlying ionization transition is shown below the PIE spectrum in green. The downward arrow indicates the calculated adiabatic IE, the lowest energy origin transition. **b).** Calculated Ce_3O_6 structures (Ce is white and O is red) and ionization processes. Ionization transitions are shown as coloured arrows which correspond to their respective ZEKE spectra. The **^{2}XIIA$^+$** and **^{2}XIIB$^+$** structures are shown for completeness only.

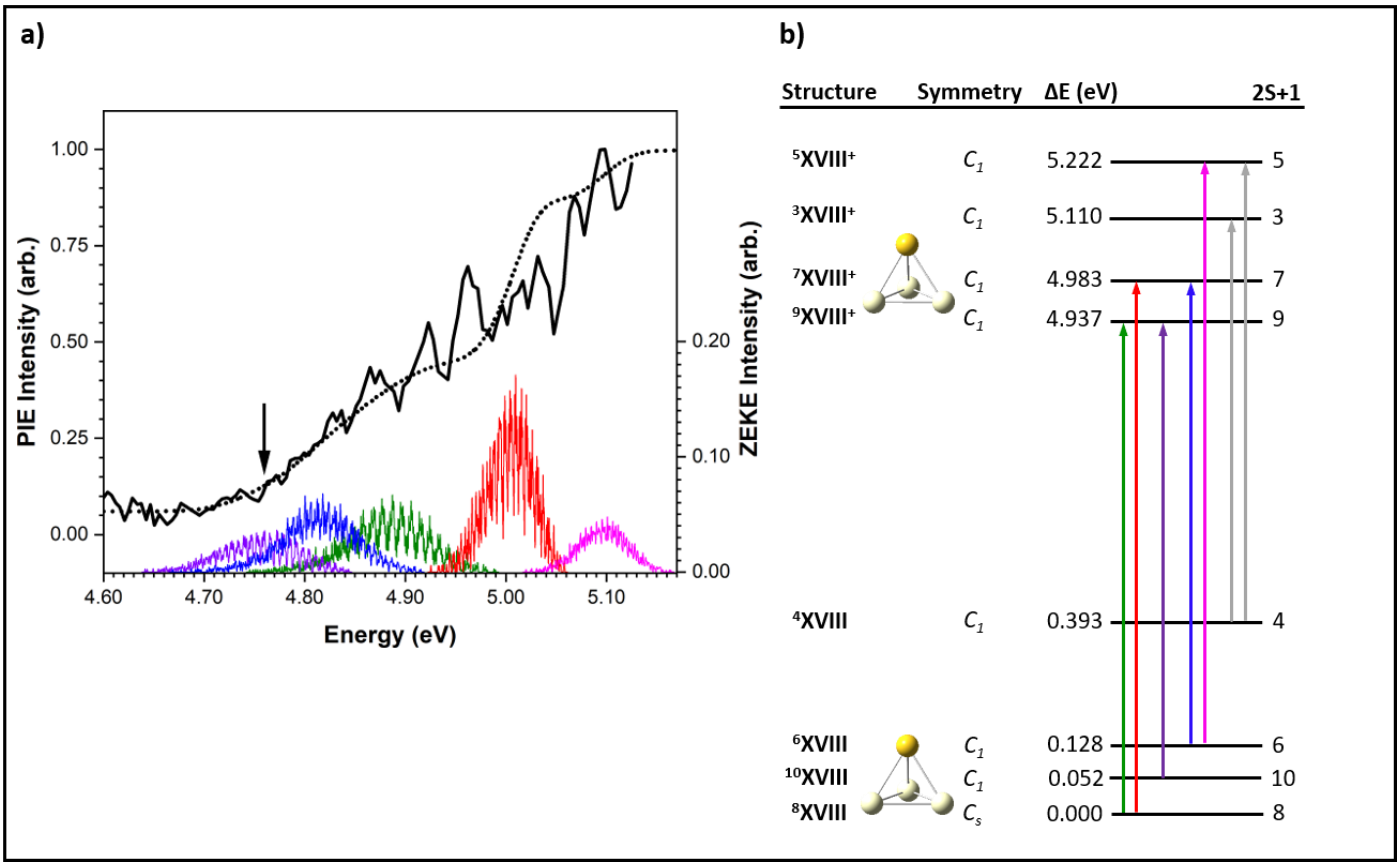

Figure S9: a). PIE spectrum for the $AuCe_3$ cluster. Experimentally recorded and calculated PIE spectra are shown as solid and dotted black lines, respectively. Calculated ZEKE spectra for underlying ionization transitions are shown below the PIE spectra in green, red, purple, blue and magenta. The downward arrow indicates the adiabatic IE, the lowest energy origin transition. **b).** Calculated $AuCe_3$ structures (Au is yellow and Ce is white) and ionization processes. Ionization transitions are shown as coloured arrows which correspond to their respective ZEKE spectra. Ionization processes not considered to contribute to the PIE spectrum – due to energetically unfavourable neutral species - are shown as solid grey arrows.

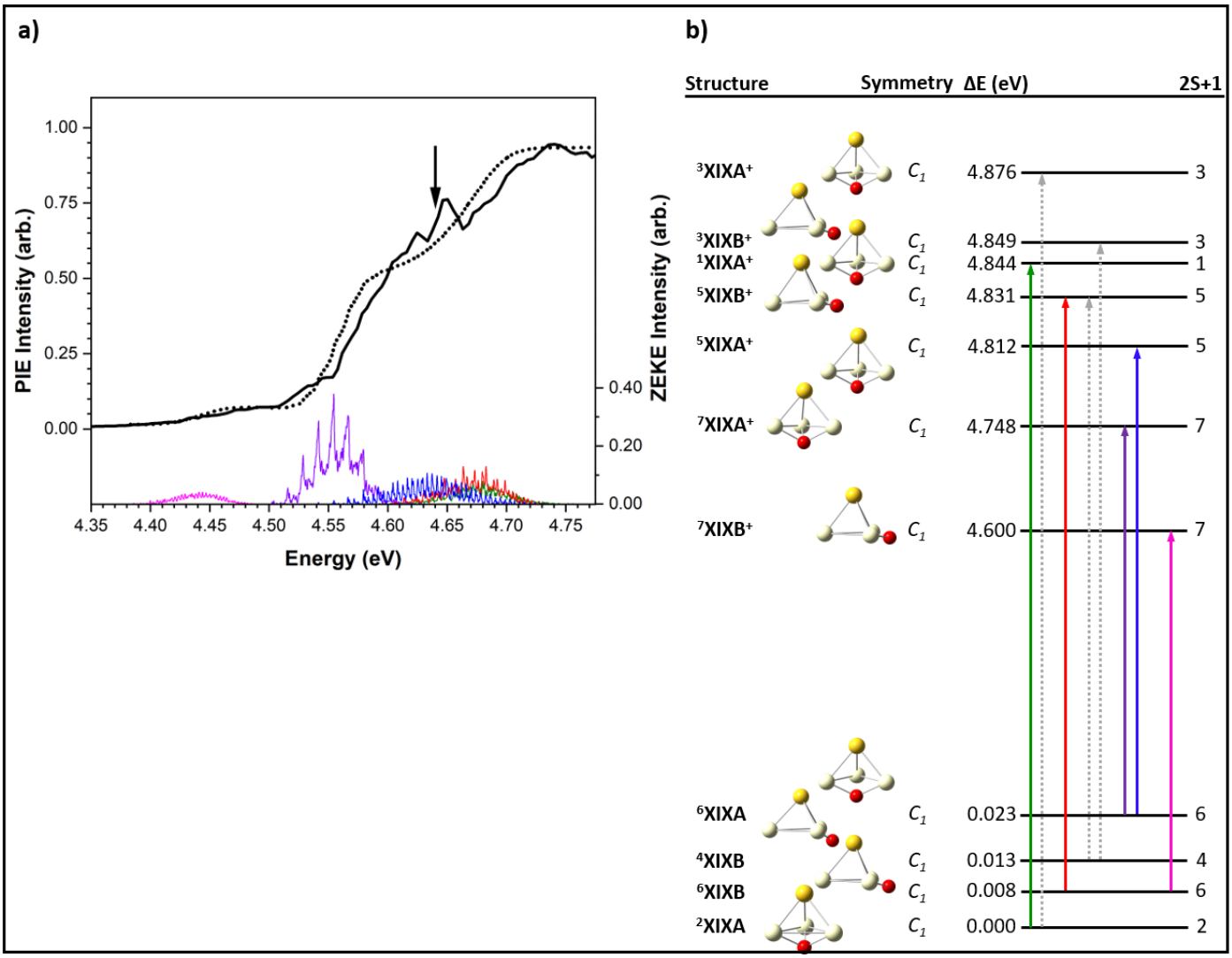

Figure S10: a). PIE spectrum for the $AuCe_3O$ cluster. Experimentally recorded and calculated PIE spectra are shown as solid and dotted black lines, respectively. Calculated ZEKE spectra for underlying ionization transitions are shown below the PIE spectra in green, red, violet, blue and magenta. The downward arrow indicates the adiabatic IE, the lowest energy origin transition. **b).** Calculated $AuCe_3O$ structures (Au is yellow, Ce is white and O is red) and ionization processes. Ionization transitions are shown as coloured arrows which correspond to their respective ZEKE spectra. Ionization processes not considered to contribute to the PIE spectrum – due to weak FC overlap - are shown as dotted grey arrows.

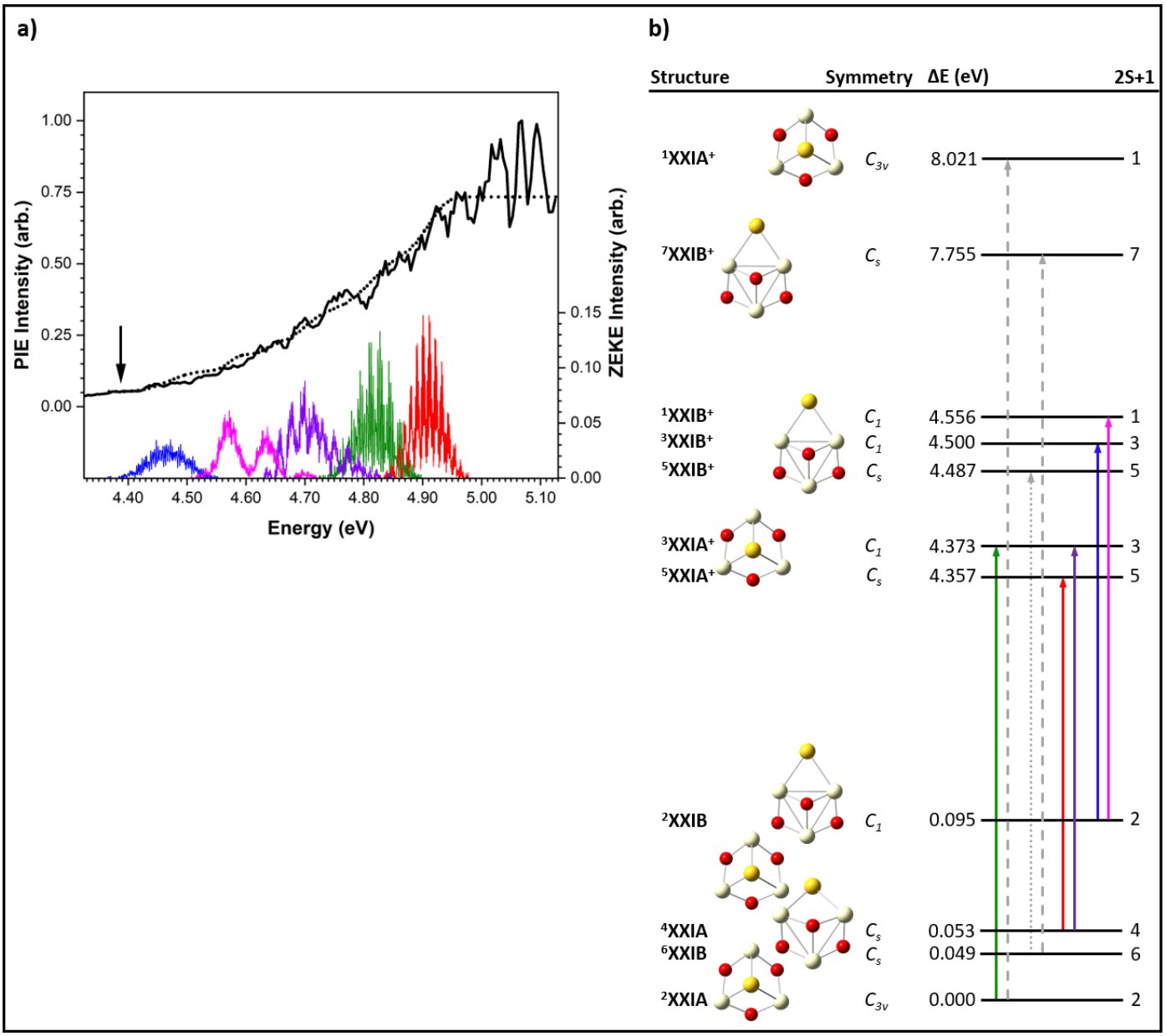

Figure S11: a). PIE spectrum for the $AuCe_3O_3$ cluster. Experimentally recorded and calculated PIE spectra are shown as solid and dotted black lines, respectively. Calculated ZEKE spectra for underlying ionization transitions are shown below the PIE spectra in green, red, violet, blue and magenta. The downward arrow indicates the adiabatic IE, the lowest energy origin transition. **b).** Calculated $AuCe_3O_3$ structures (Au is yellow, Ce is white and O is red) and ionization processes. Ionization transitions are shown as coloured arrows which correspond to their respective ZEKE spectra. Ionization processes not considered to contribute to the PIE spectrum – due to high ionization energies and weak FC overlap - are shown as dashed grey arrows and dotted grey arrows, respectively.

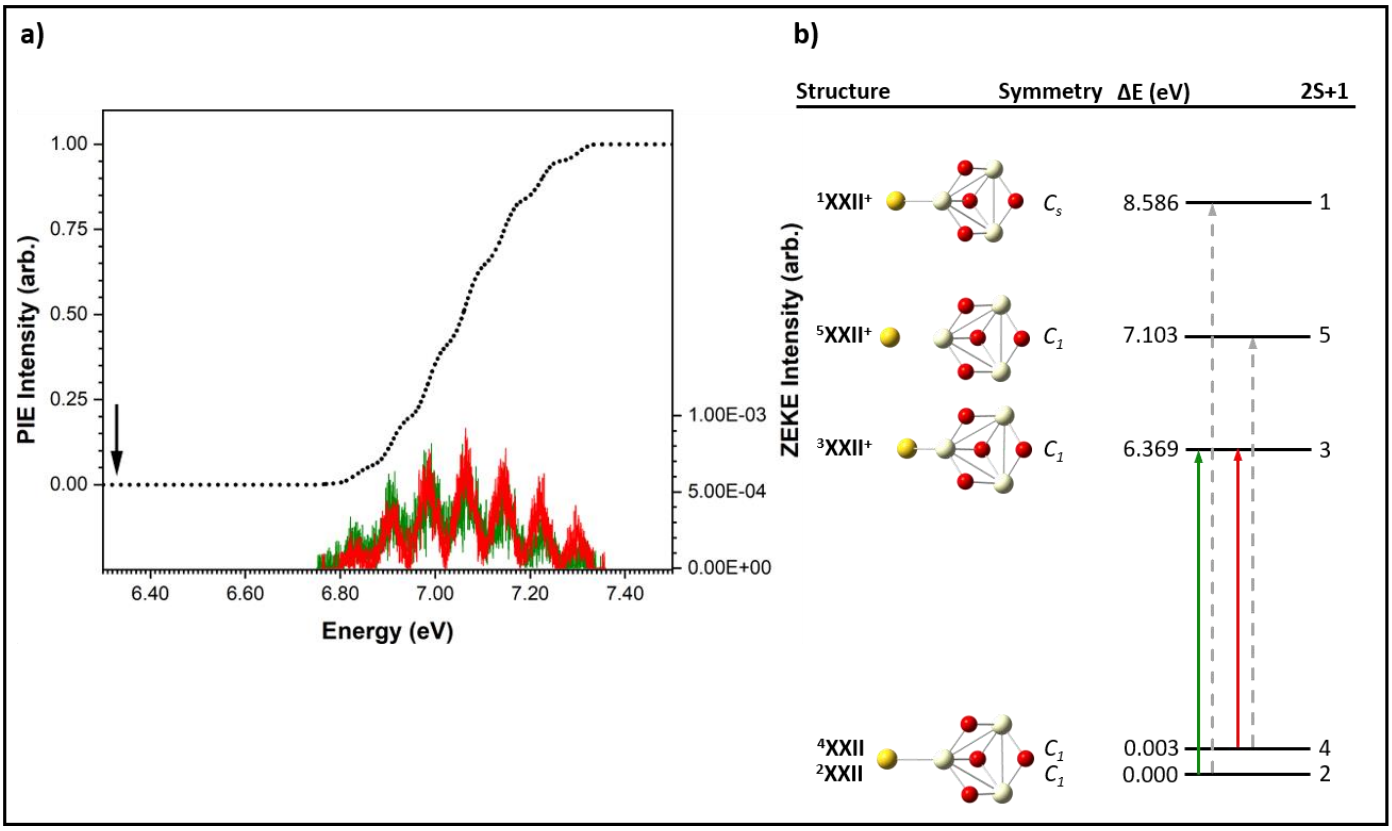

Figure S12: a). PIE spectrum for the $AuCe_3O_4$ cluster. The calculated PIE spectrum is shown as a dotted black line. Calculated ZEKE spectra for underlying ionization transitions are shown below the PIE spectra in green and red. The downward arrow indicates the calculated adiabatic IE, the lowest energy origin transition. **b).** Calculated $AuCe_3O_4$ structures (Au is yellow, Ce is white and O is red) and ionization processes. Ionization transitions are shown as coloured arrows which correspond to their respective ZEKE spectra. Ionization processes not considered to contribute to the PIE spectrum – due to high ionization energies - are shown as dashed grey arrows.

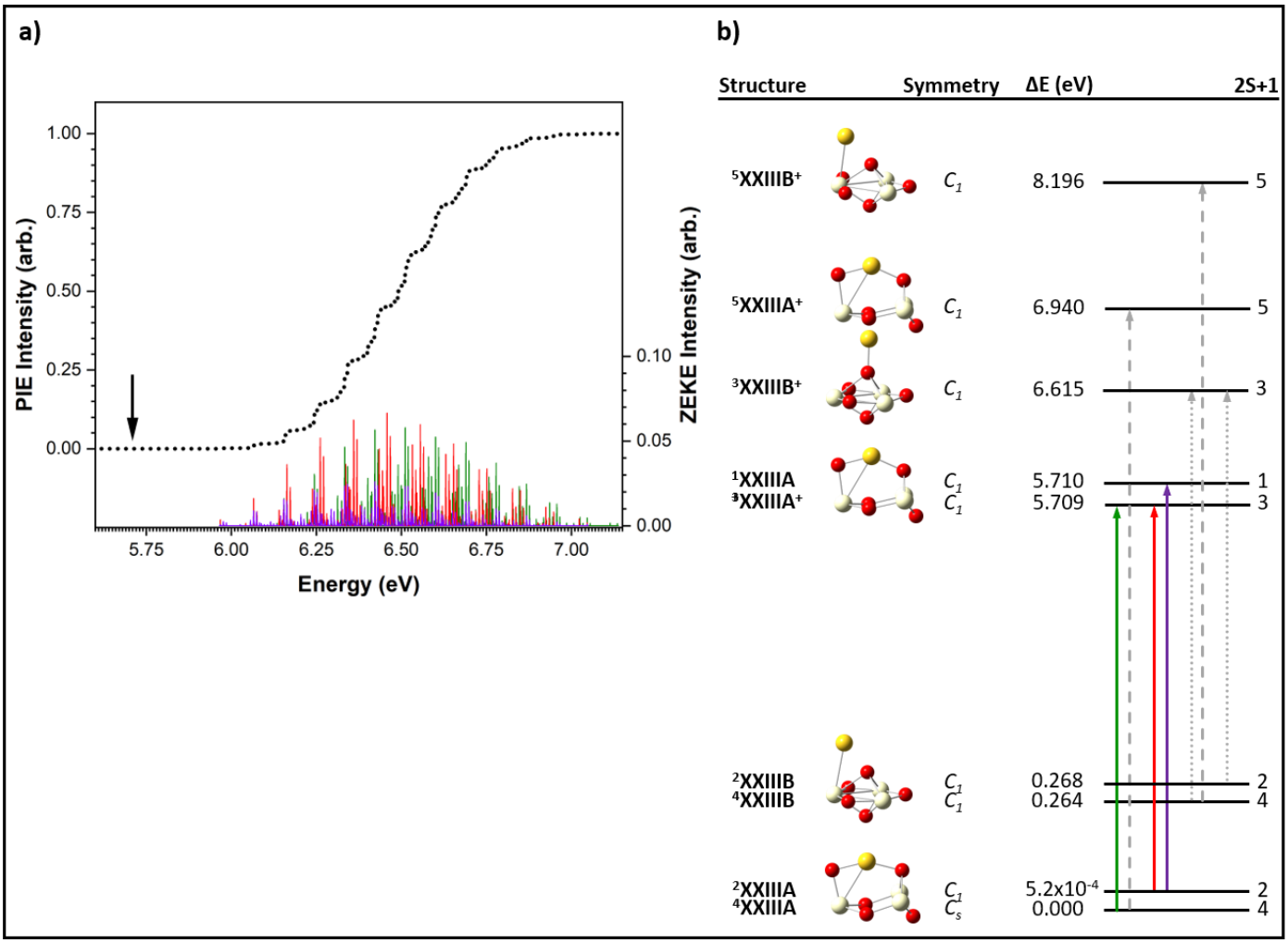

Figure S13: a). PIE spectrum for the $AuCe_3O_5$ cluster. The calculated PIE spectrum is shown as a dotted black line. Calculated ZEKE spectra for underlying ionization transitions are shown below the PIE spectra in green, red and violet. The downward arrow indicates the calculated adiabatic IE, the lowest energy origin transition. **b).** Calculated $AuCe_3O_5$ structures (Au is yellow, Ce is white and O is red) and ionization processes. Ionization transitions are shown as coloured arrows which correspond to their respective ZEKE spectra. Ionization processes not considered to contribute to the PIE spectrum – due to high ionization energies and weak FC overlap - are shown as dashed grey arrows and dotted grey arrows, respectively.

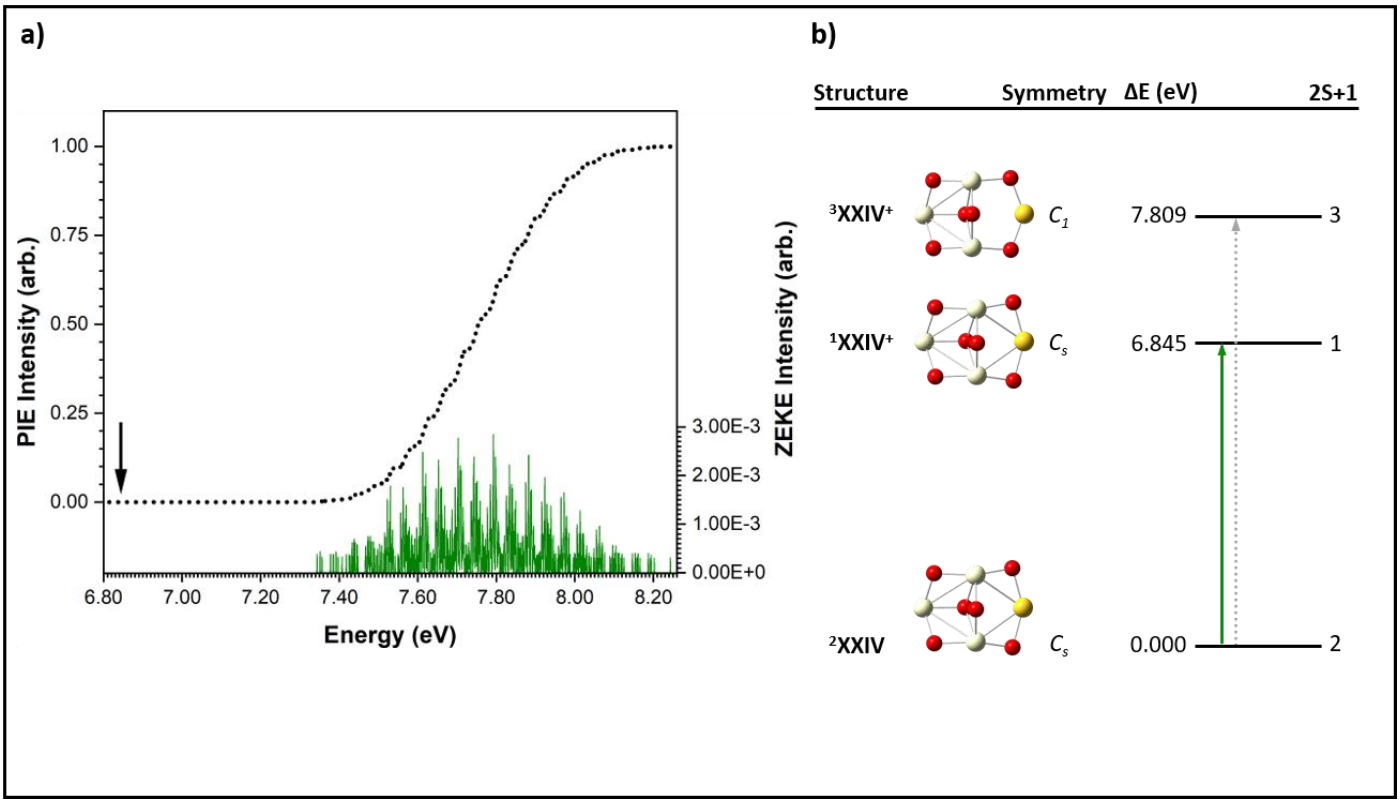

Figure S14: a). PIE spectrum for the $AuCe_3O_6$ cluster. The calculated PIE spectrum is shown as a dotted black line. The calculated ZEKE spectrum for the underlying ionization transition is shown below the PIE spectrum in green. The downward arrow indicates the calculated adiabatic IE, the lowest energy origin transition. **b).** Calculated $AuCe_3O_6$ structures (Au is yellow, Ce is white and O is red) and ionization processes. Ionization transitions are shown as coloured arrows which correspond to their respective ZEKE spectra. Ionization processes not considered to contribute to the PIE spectrum – due to weak FC overlap - are shown as dotted grey arrows.

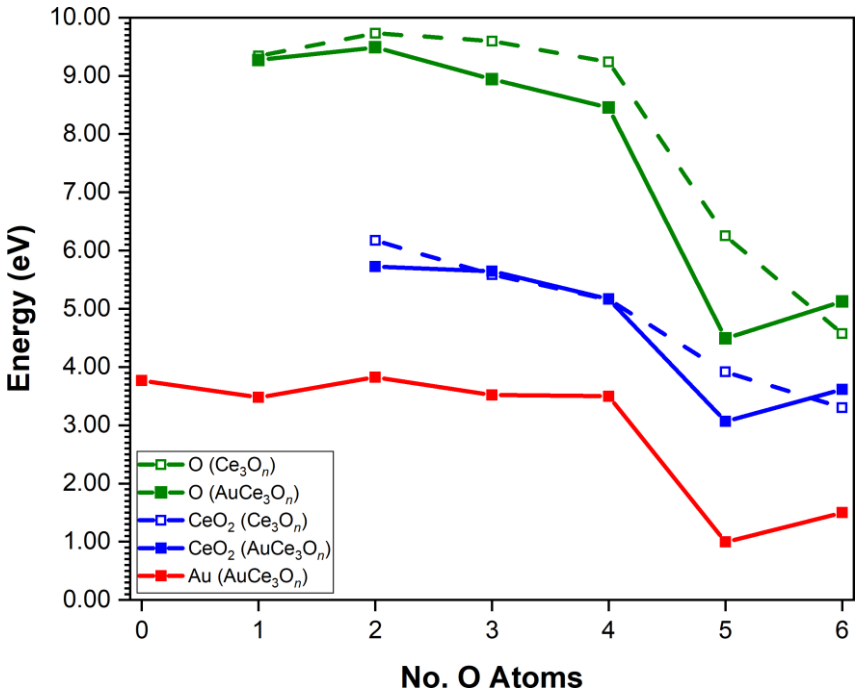

Figure S15: Calculated Au (red), O (green) and CeO_2 (blue) bonding energies for neutral Ce_3O_n (dashed line) and $AuCe_3O_n$ (solid line) clusters.

Ce_3

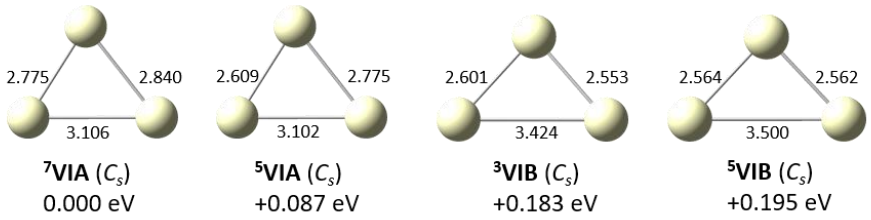

^{7}VIA (C_s) 0.000 eV
^{5}VIA (C_s) +0.087 eV
^{3}VIB (C_s) +0.183 eV
^{5}VIB (C_s) +0.195 eV

Ce_3^+

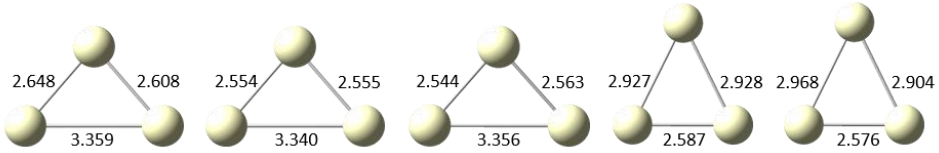

^{6}VIB$^+$ (C_s) +4.482 eV
^{2}VIB$^+$ (C_s) +4.852 eV
^{4}VIB$^+$ (C_s) +4.864 eV
^{8}VIA$^+$ (C_s) +4.966 eV
^{6}VIA$^+$ (C_s) +5.103 eV

Figure S16: Calculated Ce_3 neutral and cationic structures. Bond lengths are presented in Å. Point groups are shown in brackets. Energies are shown relative to the lowest energy neutral structure.

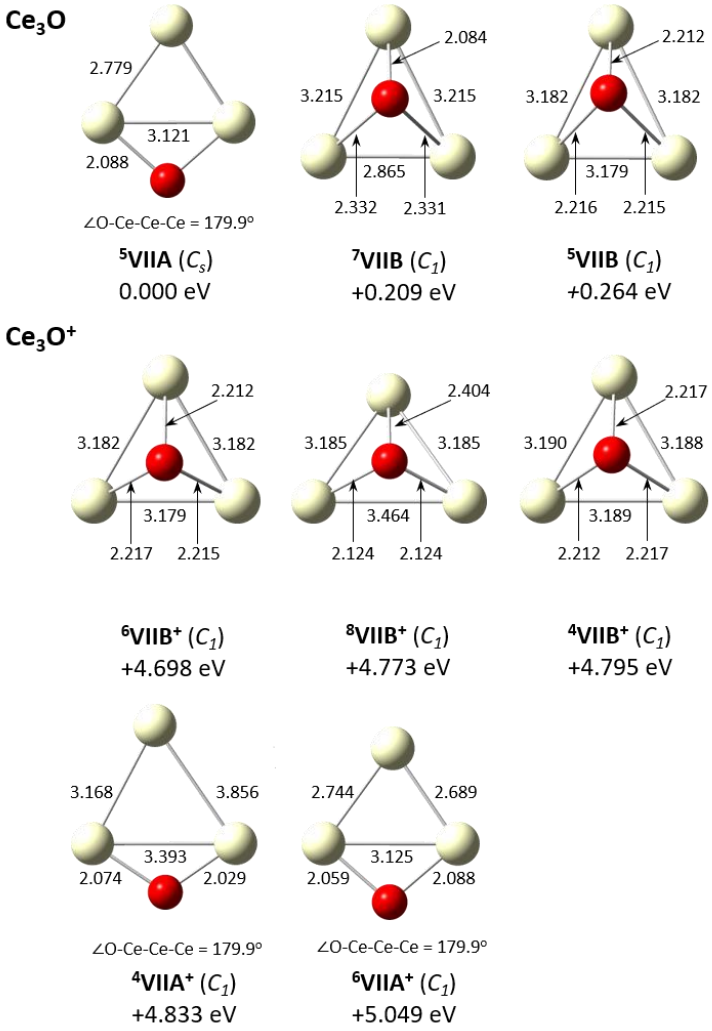

Figure S17: Calculated Ce_3O neutral and cationic structures. Bond lengths are presented in Å. Point groups are shown in brackets. Energies are shown relative to the lowest energy neutral structure.

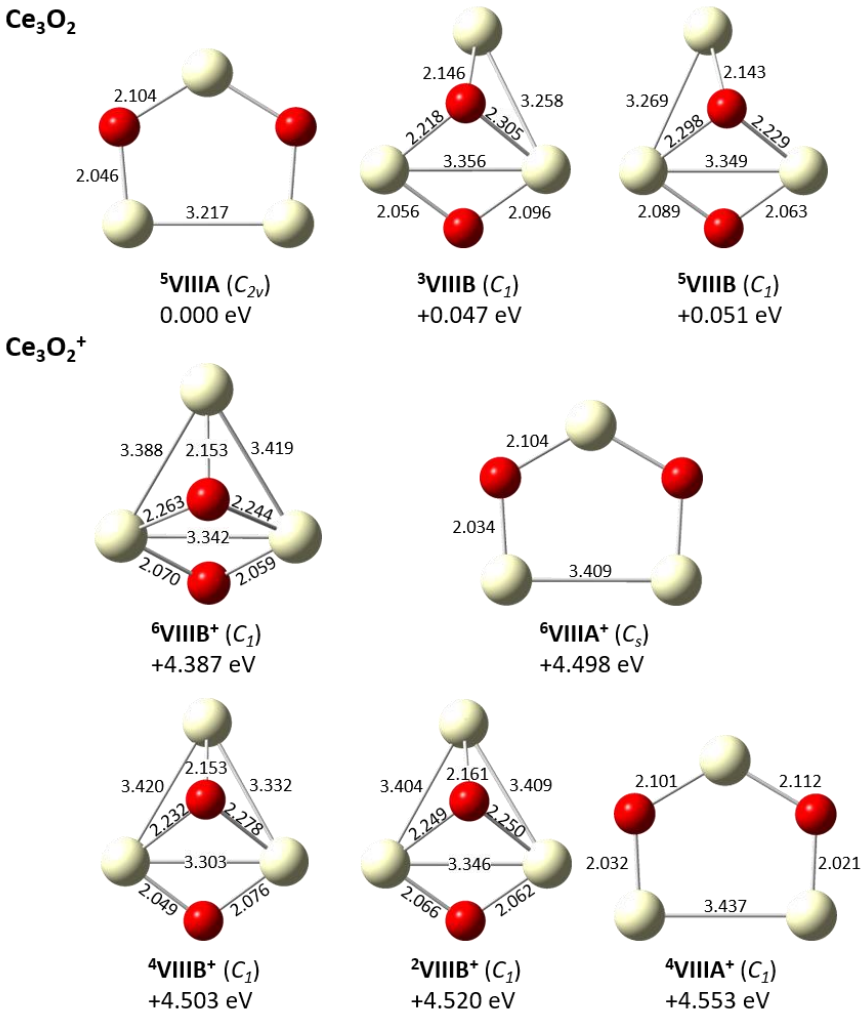

Figure S18: Calculated Ce_3O_2 neutral and cationic structures. Bond lengths are presented in Å. Point groups are shown in brackets. Energies are shown relative to the lowest energy neutral structure.

Ce_3O_3

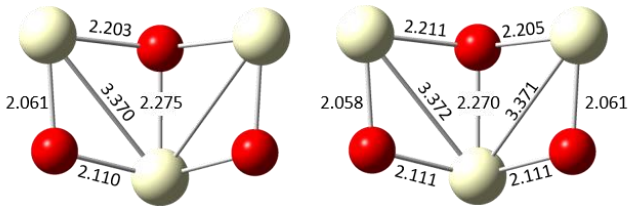

∠Ce-O-Ce = 118.4°

^{5}IX (C_s)
0.000 eV

∠Ce-O-Ce = 117.8°

^{3}IX (C_1)
+0.016 eV

$Ce_3O_3^+$

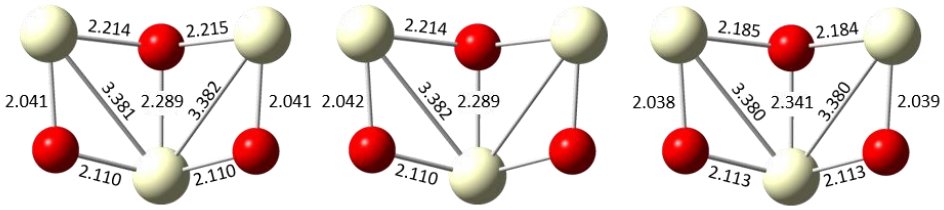

∠Ce-O-Ce = 104.9°

^{2}IX$^+$ (C_1)
+4.214 eV

∠Ce-O-Ce = 104.8°

^{4}IX$^+$ (C_s)
+4.216 eV

∠Ce-O-Ce = 132.5°

^{6}IX$^+$ (C_1)
+4.600 eV

Figure S19: Calculated Ce_3O_3 neutral and cationic structures. Bond lengths are presented in Å. Point groups are shown in brackets. Energies are shown relative to the lowest energy neutral structure.

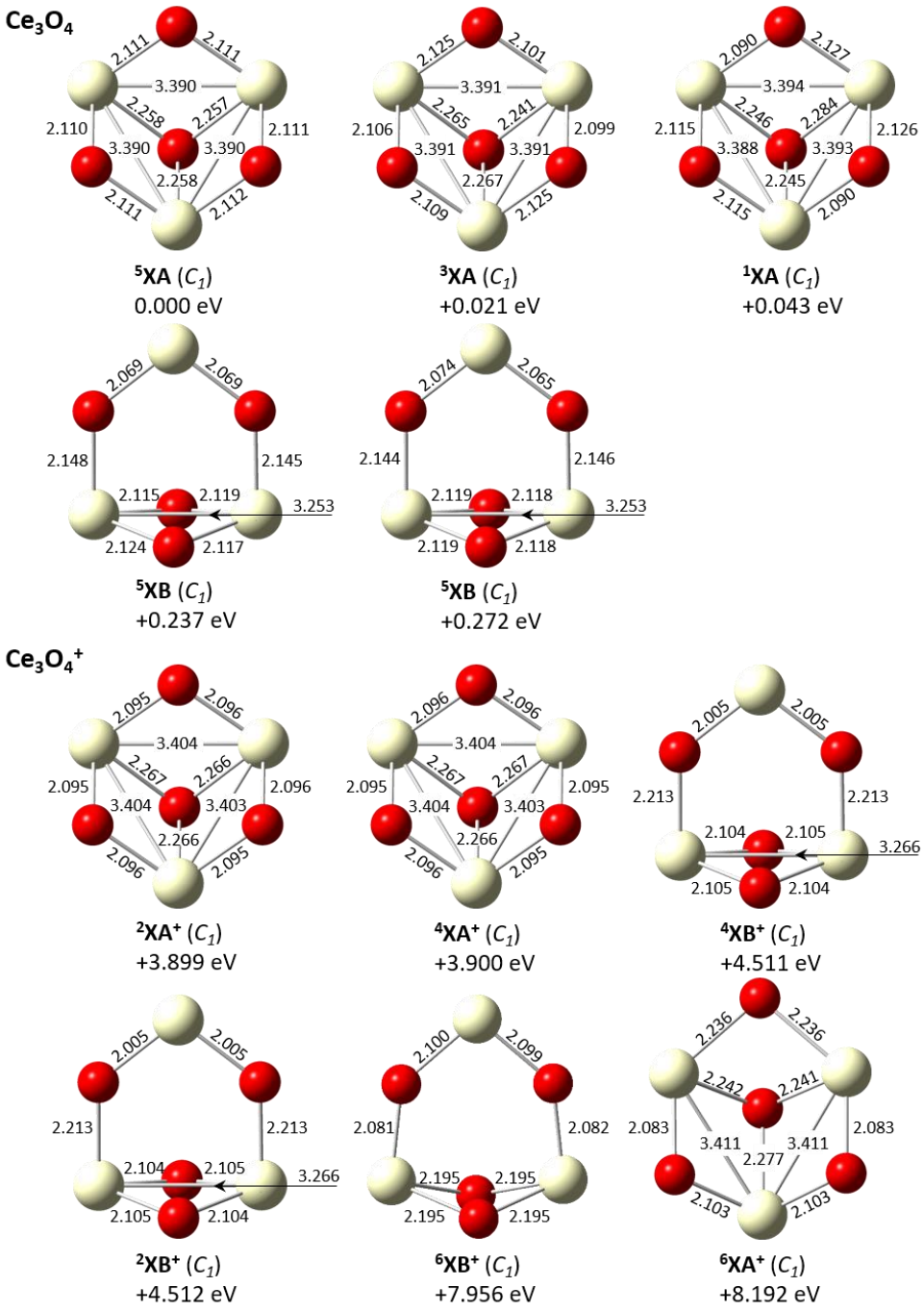

Figure S20: Calculated Ce_3O_4 neutral and cationic structures. Bond lengths are presented in Å. Point groups are shown in brackets. Energies are shown relative to the lowest energy neutral structure.

Ce_3O_5

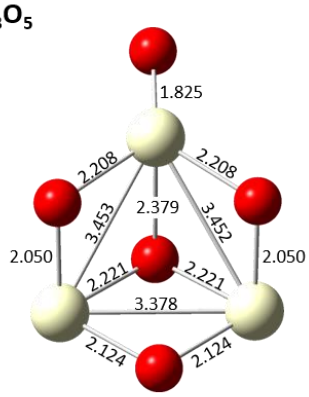

^{3}XIA (C_1)
0.000 eV

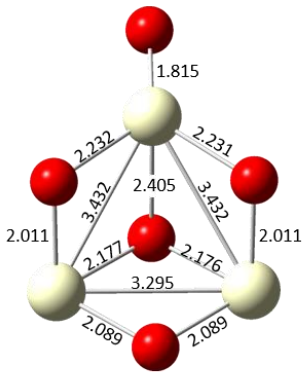

^{1}XIA (C_1)
+0.120 eV

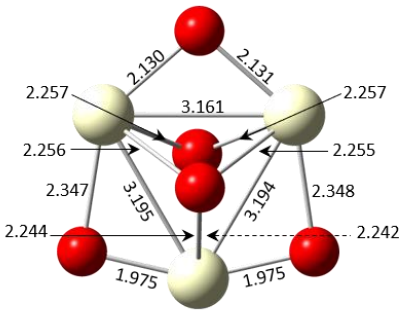

^{3}XIB (C_1)
+0.121 eV

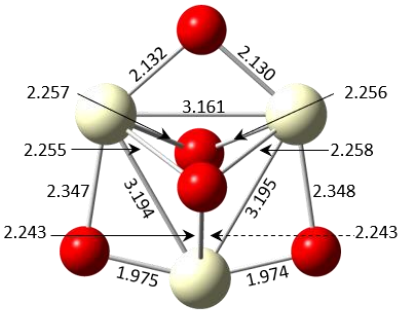

^{1}XIB (C_1)
+0.149 eV

$Ce_3O_5^+$

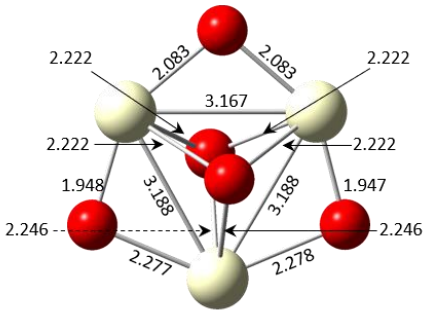

^{2}XIB$^+$ (C_1)
+6.142 eV

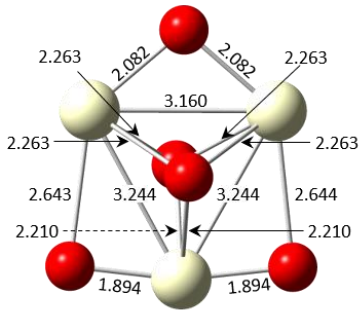

^{4}XIB$^+$ (C_1)
6.376 eV

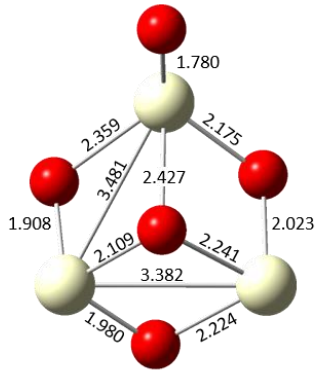

^{2}XIA$^+$ (C_1)
+7.633 eV

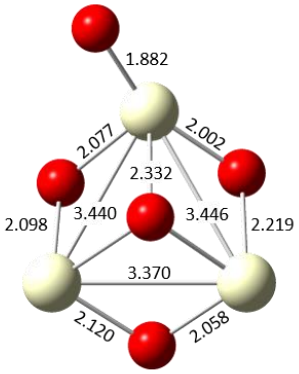

^{4}XIA$^+$ (C_1)
+8.000 eV

Figure S21: Calculated Ce_3O_5 neutral and cationic structures. Bond lengths are presented in Å. Point groups are shown in brackets. Energies are shown relative to the lowest energy neutral structure.

Ce_3O_6

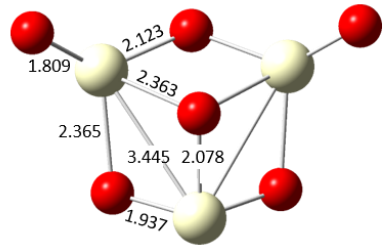

^{1}XII (C_s)
0.000 eV

$Ce_3O_6^+$

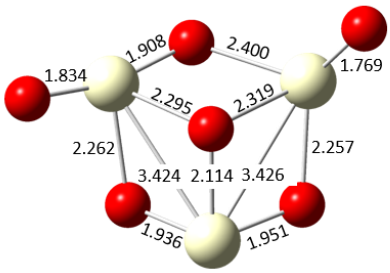

^{2}XII$^+$ (C_1)
+8.482 eV

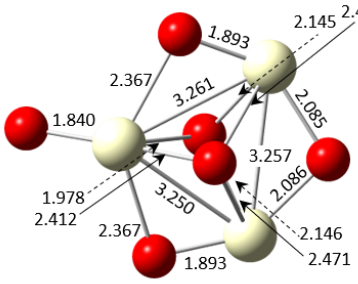

^{2}XIIA$^+$ (C_1)
+8.640 eV

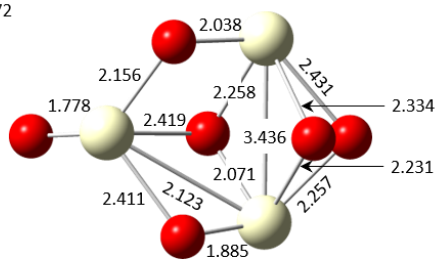

^{2}XIIB$^+$ (C_1)
+8.764 eV

Figure S22: Calculated Ce_3O_6 neutral and cationic structures. Bond lengths are presented in Å. Point groups are shown in brackets. Energies are shown relative to the lowest energy neutral structure.

$AuCe_3$

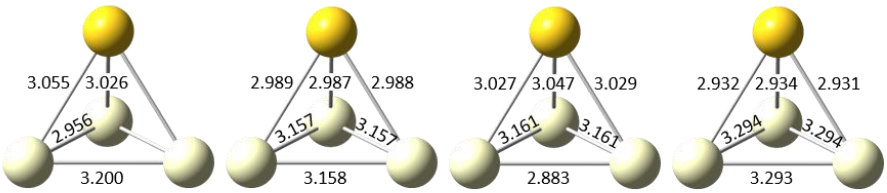

^{8}XVIII (C_s)
0.000 eV

^{10}XVIII (C_1)
+0.052 eV

^{6}XVIII (C_1)
+0.128 eV

^{4}XVIII (C_1)
+0.393 eV

$AuCe_3^+$

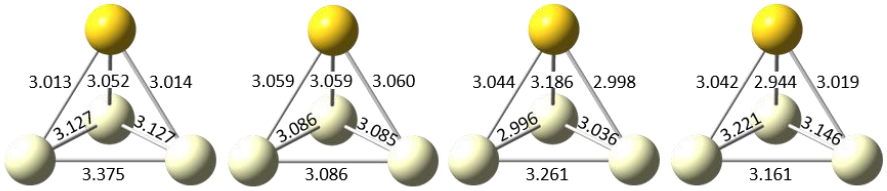

^{9}XVIII$^+$ (C_1)
+4.937 eV

^{7}XVIII$^+$ (C_1)
+4.983 eV

^{3}XVIII$^+$ (C_1)
+5.110 eV

^{5}XVIII$^+$ (C_1)
+5.222 eV

Figure S23: Calculated $AuCe_3$ neutral and cationic structures. Bond lengths are presented in Å. Point groups are shown in brackets. Energies are shown relative to the lowest energy neutral structure.

$AuCe_3O$

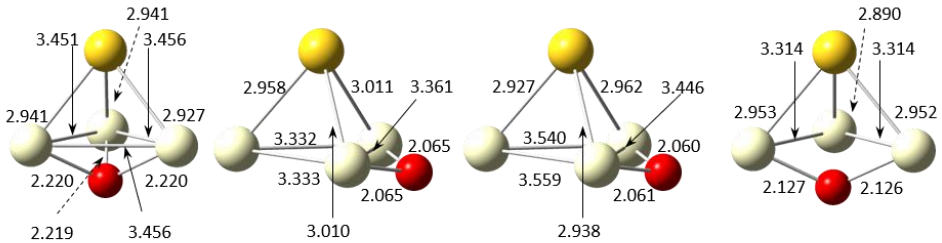

^{2}XIXA (C_1)
0.000 eV

^{6}XIXB (C_1)
+0.008 eV

^{4}XIXB (C_1)
+0.013 eV

^{6}XIXA (C_1)
+0.023 eV

$AuCe_3O^+$

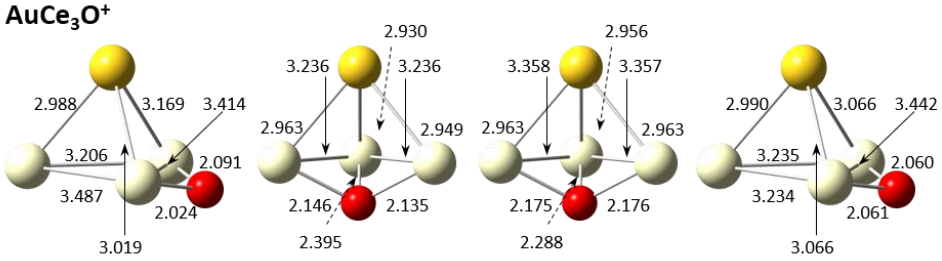

^{7}XIXB$^+$ (C_1)
+4.600 eV

^{7}XIXA$^+$ (C_1)
+4.748 eV

^{5}XIXA$^+$ (C_1)
+4.812 eV

^{5}XIXB$^+$ (C_1)
+4.831 eV

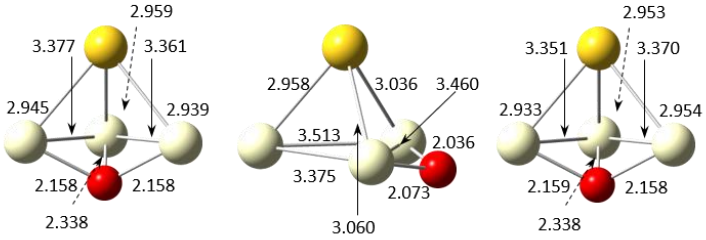

^{1}XIXA$^+$ (C_1)
+4.844 eV

^{3}XIXB$^+$ (C_1)
+4.849 eV

^{3}XIXA$^+$ (C_1)
+4.876 eV

Figure S24: Calculated $AuCe_3O$ neutral and cationic structures. Bond lengths are presented in Å. Point groups are shown in brackets. Energies are shown relative to the lowest energy neutral structure.

$AuCe_3O_2$

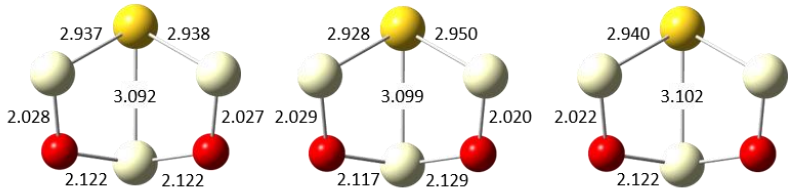

^{6}**XX** (C_1)
0.000 eV

^{4}**XX** (C_1)
+0.035 eV

^{2}**XX** (C_s)
+0.068 eV

$AuCe_3O_2^+$

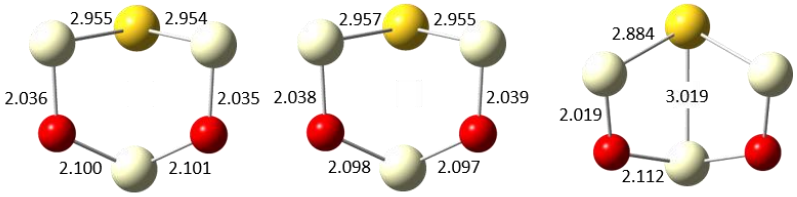

^{5}**XX**$^+$ (C_1)
+4.736 eV

^{3}**XX**$^+$ (C_1)
+4.764 eV

^{7}**XX**$^+$ (C_s)
+4.822 eV

Figure S25: Calculated $AuCe_3O_2$ neutral and cationic structures. Bond lengths are presented in Å. Point groups are shown in brackets. Energies are shown relative to the lowest energy neutral structure.

$AuCe_3O_3$

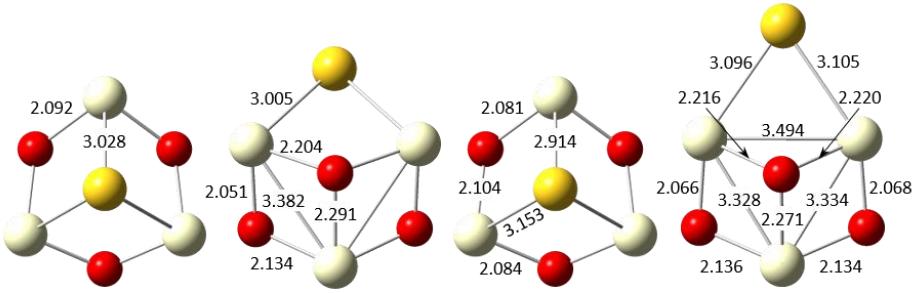

^{2}XXIA (C_{3v}) 0.000 eV

^{6}XXIB (C_s) +0.049 eV

^{4}XXIA (C_s) +0.053 eV

^{2}XXIB (C_1) +0.095 eV

$AuCe_3O_3^+$

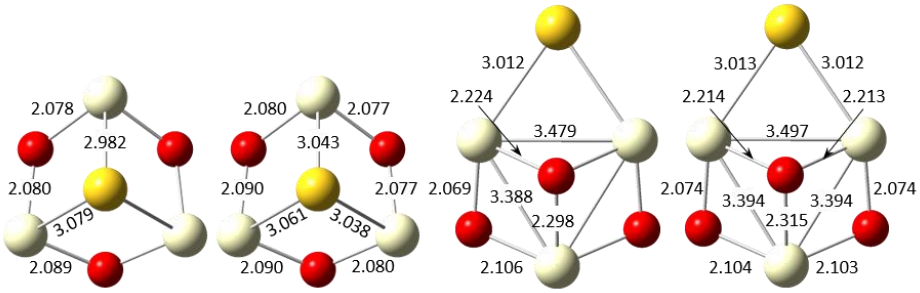

^{5}XXIA$^+$ (C_s) +4.357 eV

^{3}XXIA$^+$ (C_1) +4.373 eV

^{5}XXIB$^+$ (C_s) +4.487 eV

^{3}XXIB$^+$ (C_1) +4.500 eV

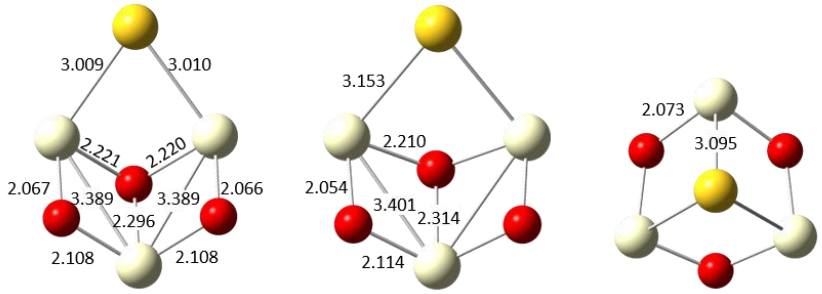

^{1}XXIB$^+$ (C_1) +4.556 eV

^{7}XXIB$^+$ (C_s) +7.755 eV

^{1}XXIA$^+$ (C_{3v}) +8.021 eV

Figure S26: Calculated $AuCe_3O_3$ neutral and cationic structures. Bond lengths are presented in Å. Point groups are shown in brackets. Energies are shown relative to the lowest energy neutral structure.

$AuCe_3O_4$

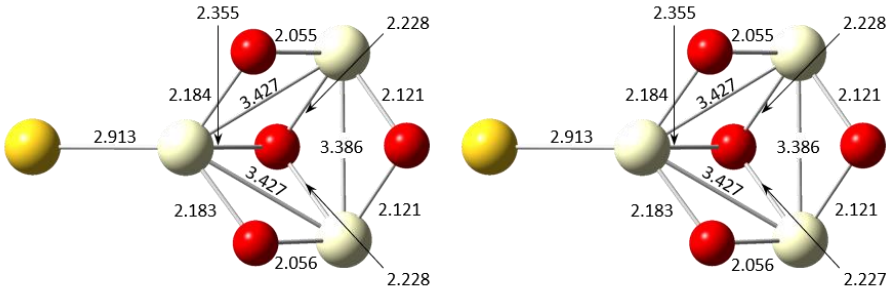

^{2}XXII (C_1)
0.000 eV

^{4}XXII (C_1)
+0.003 eV

$AuCe_3O_4^+$

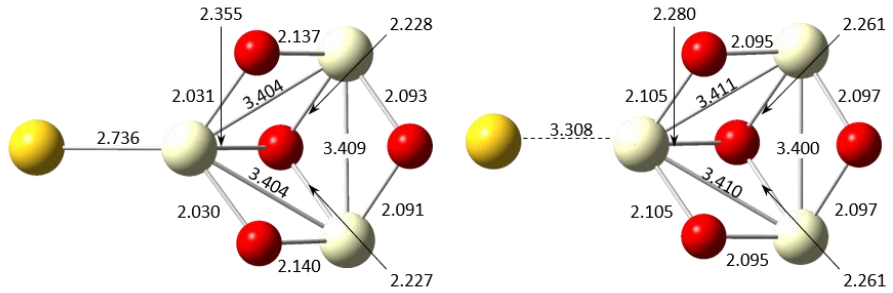

^{3}XXII$^+$ (C_1)
+6.369 eV

^{5}XXII$^+$ (C_1)
+7.103 eV

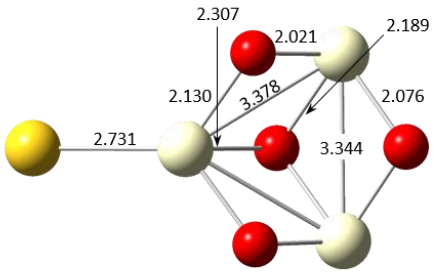

^{1}XXII$^+$ (C_s)
+8.586 eV

Figure S27: Calculated $AuCe_3O_4$ neutral and cationic structures. Bond lengths are presented in Å. Point groups are shown in brackets. Energies are shown relative to the lowest energy neutral structure.

$AuCe_3O_5$

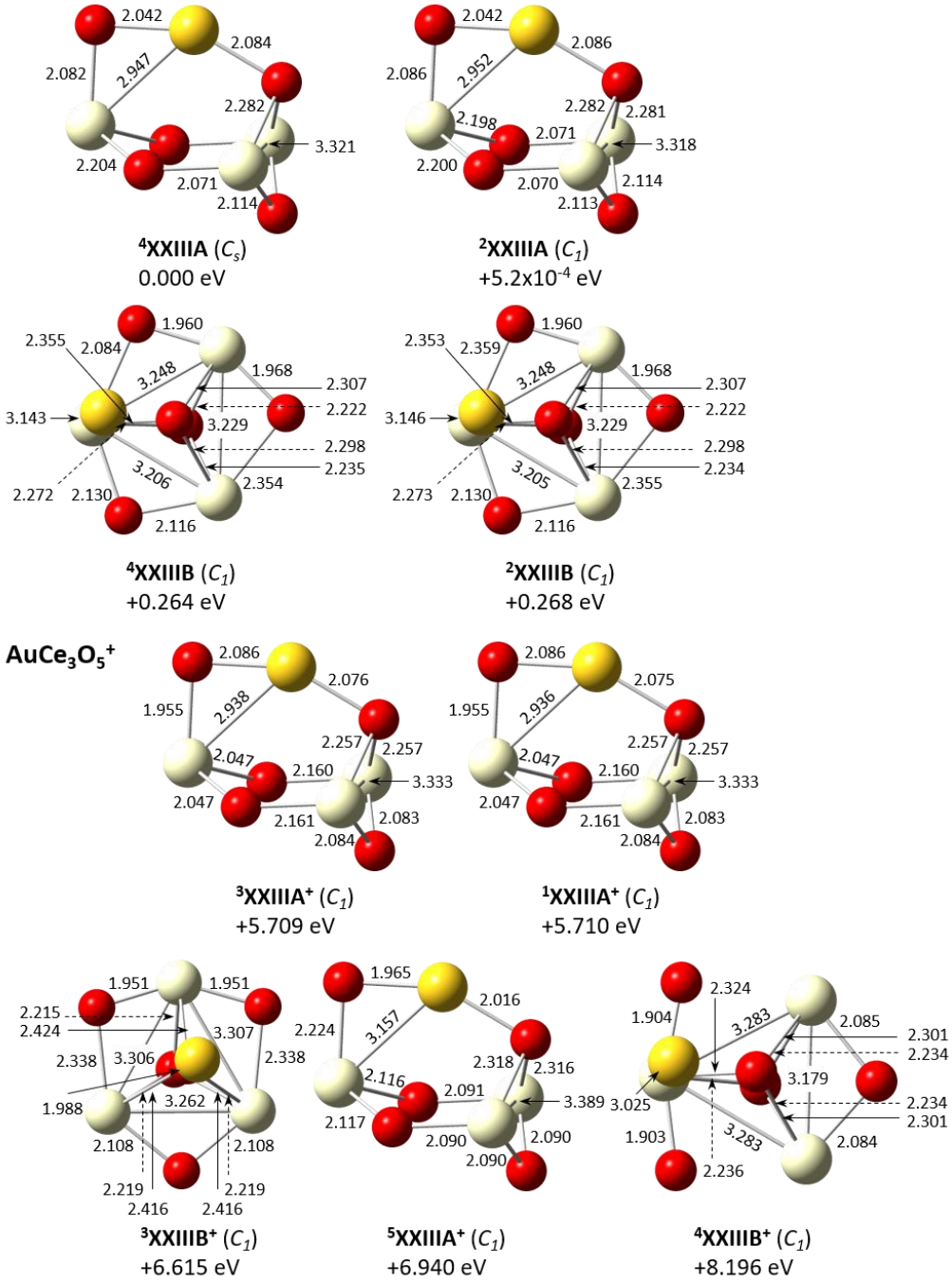

$AuCe_3O_5^+$

Figure S28: Calculated $AuCe_3O_5$ neutral and cationic structures. Bond lengths are presented in Å. Point groups are shown in brackets. Energies are shown relative to the lowest energy neutral structure.

$AuCe_3O_6$

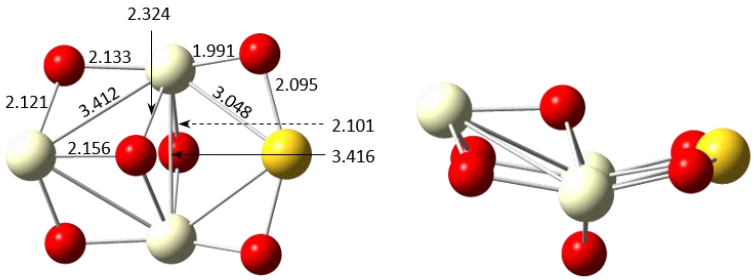

^{2}XXIV (C_s)
0.000 eV

$AuCe_3O_6^+$

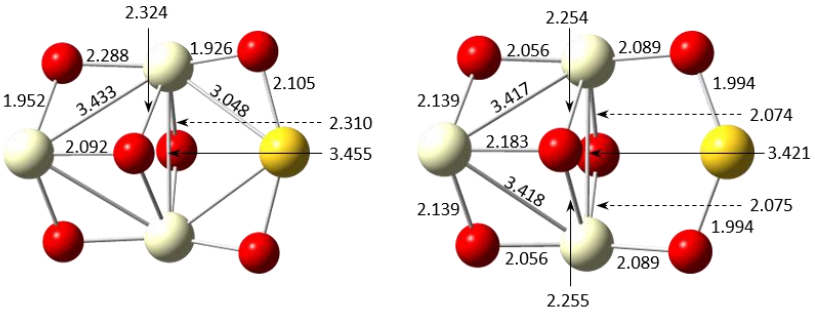

^{1}XXIV$^+$ (C_s)
+6.845 eV

^{3}XXIV$^+$ (C_1)
+7.809 eV

Figure S29: Calculated $AuCe_3O_6$ neutral and cationic structures. Bond lengths are presented in Å. Point groups are shown in brackets. Energies are shown relative to the lowest energy neutral structure.